Bull Eng Geol Environ
DOI 10.1007/s10064-015-0750-9

ORIGINAL PAPER

An integrated approach for detection and delineation of leakage path from Micro-Dam Reservoir (MDR): a case study from Arato MDR, Northern Ethiopia

Gebremedhin Berhane[1,2] · **Samuel Kebede**[1] · **Tesfamichael Gebreyohannes**[1] · **Kristine Martens**[2] · **Marc Van Camp**[2] · **Kristine Walraevens**[2]

Received: 1 November 2014 / Accepted: 16 April 2015

Abstract Water is at the center of all efforts to address food security, poverty reduction, economic growth, energy production and human health. In arid and semi-arid regions, groundwater and water harvesting structures (such as Micro-Dam Reservoirs, MDRs) play a significant role for irrigation and maintaining the sustainability of water resources. Fighting poverty and drought using construction of MDRs is becoming a common practice in Tigray (northern Ethiopia), but their implementation is not without challenges. Reservoir leakage, *inter alia*, is one of the main problems facing MDRs in the region. This paper presents geological, geophysical, hydrogeological and hydrochemical study results in MDR to better understand and delineate leakage zones and mechanisms. Conventional geological mapping, geo-electrical methods (VES and ERP), hydrogeological and geochemical methods were used to understand the geological and geo-hydrological situation of the MDR. Integrated interpretation and synthesis of the data enable to delineate the leakage zone and path. The limestone-shale-marl intercalation unit that makes up the foundation and reservoir area is found to be the leaky unit due to syngenetic and epigenetic discontinuities, while the dolerite unit is relatively impervious. Installation of a cut-off wall at the upstream toe of the dam could be a possible solution to minimize the leakage problem underneath the dam foundation and left abutment/flank. As an alternative, proper utilization of the water from big diameter shallow hand dug wells from the leakage zone downstream of the MDR may be also conceived as a target without incurring additional costs of maintenance.

Keywords Electrical profiling · Geophysics · Geology · Hydrogeology · Water harvesting · Recharge · VES

✉ Gebremedhin Berhane
gmedhin_berhane@yahoo.com

1 Department of Earth Sciences, Mekelle University, P. O. Box 1202, Mekelle, Ethiopia

2 Laboratory for Applied Geology and Hydrogeology, Ghent University, Krijgslaan 281-S8, 9000 Ghent, Belgium

Introduction

Water is the most valuable and regularly used natural resource and is critical for the survival of life (Wood 2002) and providing a wide variety of ecological and social services (Döll 2009; Houben and Weihe 2010; Laio et al. 2009). As stated on GWP (2010), water is at the center of all efforts to address food security, poverty reduction, economic growth, energy production and human health. In arid and semi-arid regions, groundwater and water harvesting structures [such as Micro-Dam Reservoirs (MDRs)] play a significant role for irrigation and maintaining the sustainability of water resources (Garrido et al. 2006; Scanlon et al. 2006). Shortage of water in Ethiopia is a serious issue and the problem is more severe in arid and semi-arid areas like northern, northeastern and eastern Ethiopia. Population growth and erratic and torrential nature of the rainfall exacerbates the problem and increases drought frequency in the region. Using groundwater and MDRs for irrigation and other purposes in these regions of Ethiopia has recently been put in place to fight poverty and secure food sufficiency.

An intensive water resource development can have a crucial role in the economic and social development of the country and in alleviating drought. In order to alleviate the problem of recurrent drought and household food security, the government of Ethiopia has taken household level water harvesting ponds, MDRs and shallow hand dug wells development as one strategy, among others, to improve the country's irrigation development (Tesfay 2007).

In northern Ethiopia, in addition to groundwater use to address the problems of recurrent drought, famine and food insecurity, efforts are being made to harvest surface water runoff in micro-dams for use both in households and small-scale irrigation schemes. Over the last two decades, a number of MDRs were constructed in Tigray. As a result, substantial improvements were registered in the livelihood of the rural community (Behailu and Haile 2003) and availability of water for various uses has increased. Micro-dams are usually made of earth and stones, often with inlet–outlet pipes to irrigate from few up to hundreds of hectares, although some of them are suffering from problems like siltation, water leakage and insufficient inflow (yield) and water logging of agricultural land on their downstream (Evans et al. 2012; Berhane et al. 2013; Abdulkadir 2009; Haregeweyn et al. 2006). Due to these technical and operational problems, most of the MDRs are not functioning or operating as per intended objectives (Abdulkadir 2009; Berhane 2010; Desta 2005; Gonzalez-Quijano 2006; Haregeweyn et al. 2005, 2006; Nedaw and Walraevens 2009).

The fact that Ethiopia is located in the tropics, latitude 3°N to 18°N, combined with the high range of altitude, −120 to +4650 m, and the pressure and air flow pattern determine the tremendous differences in climate which prevail in different parts of the country (Cherent 1993). As in most part of northern Ethiopia, in the study area the amount of rainfall is variable; it varies from place to place and from time to time.

The northern part of the country, particularly the area around Mekelle Outlier, is drained by intermittent rivers, which are dry 8–9 months of the year (Nedaw and Walraevens 2009) and almost only 2–3 months of the year are wet, while the remaining months are dry. About 75–80 % of the rainfall comes during the months of July and August. The hydro-meteorological condition/pattern is a clear and straightforward reason for the need of surface water harvesting structures (e.g. ponds, MDRs, medium and large dams, etc.) to ensure availability of water during the long dry months of the year. Indeed, implementation of Water Harvesting Structures (WHS) like MDRs is relevant in the semi-arid regions of the African tropics, characterized by large inter-annual changes in precipitation and river discharges, and where increasing population pressure makes areas more sensitive to the fluctuations of water resources. In response to the drought and erratic rainfall patterns that have affected this area, the Federal and regional governments have undertaken the goal to rectify these defects by implementing WHS of different types.

Earth and rock dams are designed to operate under steady state seepage. Anomalous seepage may be a threat to the integrity of the structure. In spite of advances made in the fields of engineering geology, it is not possible to have 100 % leak-proof structure (Panthulu et al. 2001). Any excessive and unplanned seepage may lead to the structural and water storage failures of the dam.

Research on reservoir leakage is an important subject in water resources, irrigation and hydropower projects (Berhane and Walraevens 2013). Understanding the performance and leakage mechanisms of the MDRs in the country is made difficult by the paucity of available data. A lack of appropriate leakage investigation and monitoring can result in repairs that are unsuccessful in controlling or reducing leakage.

This paper is aiming at assessing and evaluating the leakage paths and mechanisms using engineering geological and geo-hydrological investigations of the MDR and at identifying the main causes of the leakage. The main goal of the study was to investigate the hydraulic connection between the impounded reservoir and the downstream seepage/leakage discharge zone, and to provide a plausible explanation and solution to the problem.

Regional geological and hydrogeological setting

Several authors investigated the geology of Ethiopia in general and northern Ethiopia in particular (Alene et al. 2006; Arkin et al. 1971; Asrat et al. 2001, 2003; Beyth 1972; Bheemalingeswara and Tadesse 2009; Dow et al. 1971; Dubey et al. 2007; Garland 1980; Kazmin 1972; Levitte 1970; Tadesse 1996). Based on stratigraphic sequence, the northern Ethiopian geology can be classified (from the youngest to the oldest) as follows: Flood Basalt (Tertiary/Quaternary Volcanics), Amba Aradam (Upper Sandstone) Formation, Agula Shale Formation, Antalo Limestone Formation, Adigrat Sandstone (Lower Sandstone) Formation, Enticho Sandstone and Edaga Arbi Tillite Formation, and Upper Complex Metamorphic (Basement) rocks. Quaternary soil deposits are also present in depressions and flat landforms.

The hydrogeological conditions of the country are linked with the occurrence and distribution of the various hydrostratigraphic units, the topography, the recharge and discharge conditions which, in turn are related to the spatial and temporal variation of rainfall. These hydrostratigraphic units include the Precambrian basement, Palaeozoic and Mesozoic sedimentary rocks, Tertiary and Quaternary volcanics, and Tertiary and Quaternary sedimentary rocks and sediments (Pavelic et al. 2012).

The Mesozoic sedimentary rocks are widely distributed in the present study area (around Mekelle City). Mesozoic sedimentary rocks possess both primary and secondary permeability that play important role in the occurrence and movement of groundwater. The Mesozoic sedimentary rocks can make good aquifers when they are found under favorable climatic and topographic conditions.

Groundwater in the Mekelle Outlier is mainly associated with fracturing and joints (faults) and impact of dolerite intrusion on country rock. The major faults, joints and sedimentary bedding planes play an important role in groundwater occurrence and movement. Beyth (1971) reported that in the area there are two major fault systems, NW–SE and NE–SW trending faults.

Description of the study site

Arato MDR is located at about 35 km east of Mekelle City. It was designed with a dam height of 20 m and gross reservoir capacity of 2.59×10^6 m^3. The purpose was to harvest runoff from a catchment area of 20.7 km^2 and use the water for irrigation purposes during dry seasons. Arato MDR is a typical example of an almost abandoned irrigation scheme as a result of reservoir leakage. Figure 1 shows simplified location of Arato MDR and its surrounding. The topographic elevation of the Arato study area varies from 2400 to 2560 m.a.s.l. Arato River is the biggest river in the catchment and it flows southwards of the study area until it joins the Illala River further downstream of Arato MDR. It used to be seasonal, but nowadays, after Arato MDR was constructed, it became perennial. Seasonal tributary streams originating from the highlands are flowing towards the Arato reservoir.

In many MDRs (e.g. Tsinkanet MDR), the rivers are seasonal in the upstream, whereas perennial in the downstream, due to continuous leakage from the reservoir that recharges shallow aquifers and leads to emerging new springs and increases the discharge of existing ones (Gonzalez-Quijano 2006). This situation is also true at Arato MDR as confirmed by direct field observation. The Arato Reservoir, which entered into service in 1998, has suffered from severe leakage from the outset, preventing it

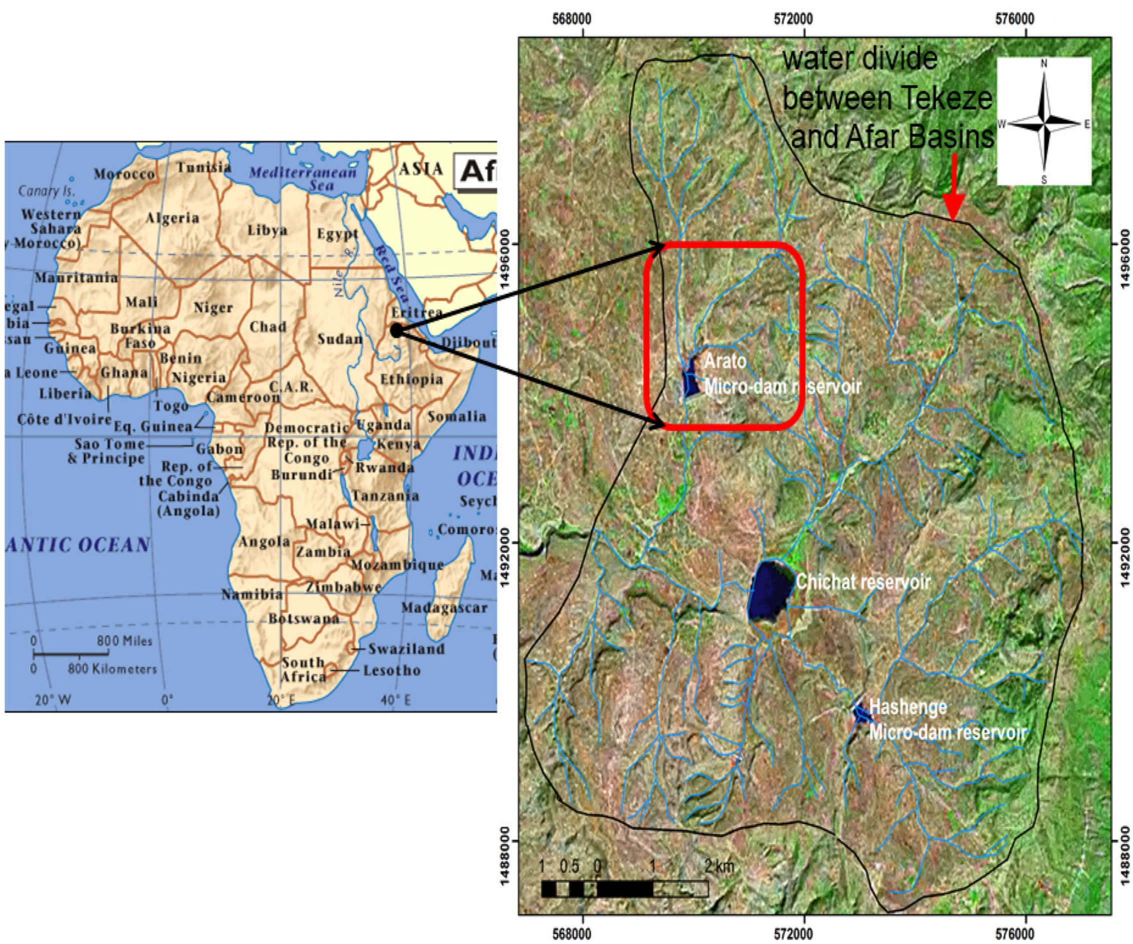

Fig. 1 Simplified location map of Arato MDR and its environs showing other MDRs in the area (colour satellite image in the background). UTM Zone 37°N coordinates

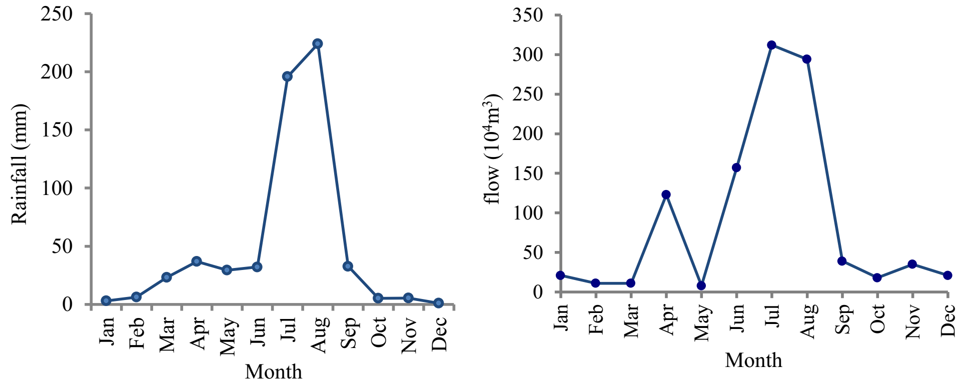

Fig. 2 Long term mean monthly rainfall (1960–2000) (*left*) and hydrograph of Illala River (1980–1986) (*right*). Location of the meteorological and Illala River gauging stations are about 15 km downstream of Arato MDR

from performing the water management functions originally foreseen for it (e.g. irrigation of about 100 ha of land). However, MDRs contribute to or enhance distributed water availability feeding shallow aquifers and streams through diffuse seepage and/or concentrated leakage. Present hydrogeophysical studies have made it possible to determine the response of the underlying Quaternary deposit and weathered bed rock aquifer into which the reservoir water is draining.

The mean annual rainfall of the region is about 762 mm (Nyssen et al. 2010) with the maximum amount recorded during July and August (Fig. 2). Generally, more than 80 % of precipitation on yearly basis is falling in the "Kiremt" (summer) season, June to September (Nyssen et al. 2005). According to Baert (2011), the seasonal temperature variation shows a cool (15–18 °C) winter from October to March followed by warm (>20 °C) spring from April to June. However, the temperature drops again in summer season.

Materials and methods

Conventional geological approach, geo-electrical prospection and hydrogeological/hydro-geochemical methods were used in the present study to characterize the site and to detect and delineate the leakage path from Arato MDR.

Geology and hydrogeology

Conventional geological fieldwork with the help of topographic map, GPS and pre-planned traverses were used to characterize local geology of the site. Description of natural outcrops, borehole logs and large diameter shallow test pits excavated for water extraction for local scale irrigation purposes were used to better understand the nature of weathering, thickness of soil profile and subsurface flow of water. A piezometric map was produced to better understand the groundwater flow system of the area. Groundwater level records were obtained from archives for 14 boreholes many of which were drilled in 2009 and field measurements in 9 shallow hand dug wells on the 21st of November 2014. To produce the groundwater contour map initially ArcGIS (version 9.3) software was used but later manually modified to fit with the geology and drainage system of the area.

Geophysics

Subsurface information gathered by drilling test holes are time consuming, expensive, data represents a single location, and lateral changes must be estimated or interpolated between distant points (Massoud et al. 2010). Surface geophysical methods, on the other hand, used in combination with strategic test drilling, provide more complete areal coverage than test drilling alone. Of all surface geophysical methods, the electrical resistivity method has been applied most commonly for groundwater investigations (Coker 2012; Sharma and Baranwal 2005; Telford et al. 1990) and identify zones of anomalous seepage or leakage (Bedrosian et al. 2012 and references therein; Panthulu et al. 2001; Rønning et al. 2014; Srinivasamoorthy et al. 2014).

By inducing an electrical current into the ground, the earth resistivity can be measured (Telford et al. 1990). Direct current is passing into the ground through a pair of current electrodes (*A* and *B*) and the resulting potential measurement over a pair of potential electrodes (*M* and *N*) is recorded. The resistivity of the subsurface formation observed is a function of the magnitude of the current, the recorded potential difference and the geometry of the electrode array that was used. Using SAS Terrameter (signal averaging system) 2000 produced by the Swedish company ABEM, for each electrode configuration the resistance (*R*) was measured for a volume of earth material within the electrical space. Thus, it is possible to determine the apparent resistivity (ρ_a) using Eqs. 1 and 2 (Telford et al. 1990; Lowrie 2007).

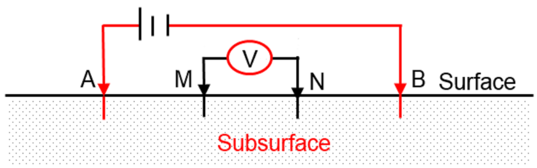

Fig. 3 Collinear four-electrode array used in resistivity surveying (A and B are current/injection electrodes and M and N are potential/ measuring electrodes)

$$\rho_a = \frac{K\Delta V}{I} \quad (1)$$

in which

$$K = 2\pi\left[\left(\frac{1}{AM} - \frac{1}{BM}\right) - \left(\frac{1}{AN} - \frac{1}{BN}\right)\right]^{-1} \quad (2)$$

K is the geometric factor for AMNB collinear four electrodes (Fig. 3), that depends on the electrode configuration:

$$K = \pi\left[\frac{L^2 - l^2}{4l}\right] \quad \text{(for Schlumberger array)}. \quad (3)$$

$$K = 2\pi a \quad \text{(for Wenner array)} \quad (4)$$

where L is separation between current electrodes and l is separation between potential electrodes (Schlumberger), a is separation between each pair of successive electrodes, which is equal for Wenner array; I is amount of electric current injected into the ground through the current electrodes A and B and ΔV is the electric potential difference between electrodes M and N.

The sounding measurements with Schlumberger array were started with an electrode spacing of 3 m and increased systematically up to 660 m, with fixed measuring centre, electrical profiling with Wenner array, fixed electrode spacings of 20 or 40 m were used, moving the measuring centre at each measurement with an interval of 20 m.

A total of 8 vertical electrical sounding (VES) using Schlumberger array were conducted, and 6 electrical resistivity profilings (ERP) using Wenner array with $a = 20$ m and $a = 40$ m for profile lines AP1, AP2, AP3 and AP4, while for AP5 and AP6, $a = 40$ m only. The ERP measurements were taken at an interval of 10 m ($X = 10$ m). Modelling of VES results was done using the IPI2win IP software developed by Bobachow (2002), utilizing the inversion modeling procedure. It gives the formation resistivity and thicknesses of the subsurface electrical layers beneath the sounding point or station.

Hydro-geochemistry

Three water samples collected on the 23rd of January, 2012, from the reservoir (Reservoir), a nearby downstream shallow hand dug well (ASHDW) and the stream (Stream) (Fig. 4) were analyzed for major cations and anions at the Laboratory for Applied Geology and Hydrogeology of Ghent University, Belgium. Major cations (Ca^{2+}, Mg^{2+}, Na^{+} and K^{+}) were determined by a Flame Technique in a High Resolution Continuum Source AAS and anions (Cl^{-}, SO_4^{2-} and NO_3^{-}) were determined by using Ion Chromatography, while HCO_3^{-} was determined using titration. In addition two hydro-geochemical analysis results from boreholes (SHW37 and BH80; Fig. 4) in the surrounding of Arato MDR were collected from archives of Tigray Water Resources Bureau (TWRB) to compare with unaffected groundwater. The reliability of the chemical analyses was verified by using an ionic balance error equation (Appelo and Postma 2005). The values were within ±5 %; hence, suitable for geochemical interpretations.

Results and discussion

Geology and geohydrology

To understand site specific features of geology and geohydrology a series of field campaigns were conducted in the area. Simplified geological map of the area is shown in Figs. 4 and 5. The foundation and reservoir are covering with three main lithological units: Quaternary deposits, Dolerite and Agula Shale (limestone-shale-marl intercalation). The Quaternary deposit within the reservoir was partly removed as construction material for the dam. This construction activity results exposure of the dolerite and limestone-shale-marl intercalation units.

Geological features such as lithology and structure control the ease with which water will flow through the ground. Based on well log data from the surrounding of the site (Kassa 2011), the main aquifers in the area are fractured or jointed and karstified limestone, and weathered and fractured dolerite and limestone-shale-marl intercalation. Except for the Quaternary deposits, the aquifer system in the area is generally due to secondary porosity and permeability. The dominant aquifer is the limestone-shale-marl intercalation unit, whereby weathered, fractured and karstified limestone forms the main water-bearing zones in the area. The water level measurements obtained from different wells with pumping test data and logs in the area suggest confined and unconfined aquifers (Kassa 2011). This is explained by the interlayering of shale in between the productive layers which acts as an aquitard.

Quaternary deposits

Quaternary deposits are exposed at flat slopes both upstream and downstream of the Arato MDR derived from nearby dolerite and limestone-shale-marl intercalation. The thickness varies from place to place from half a meter up to 5 m. The grain size of this lithological unit ranges from

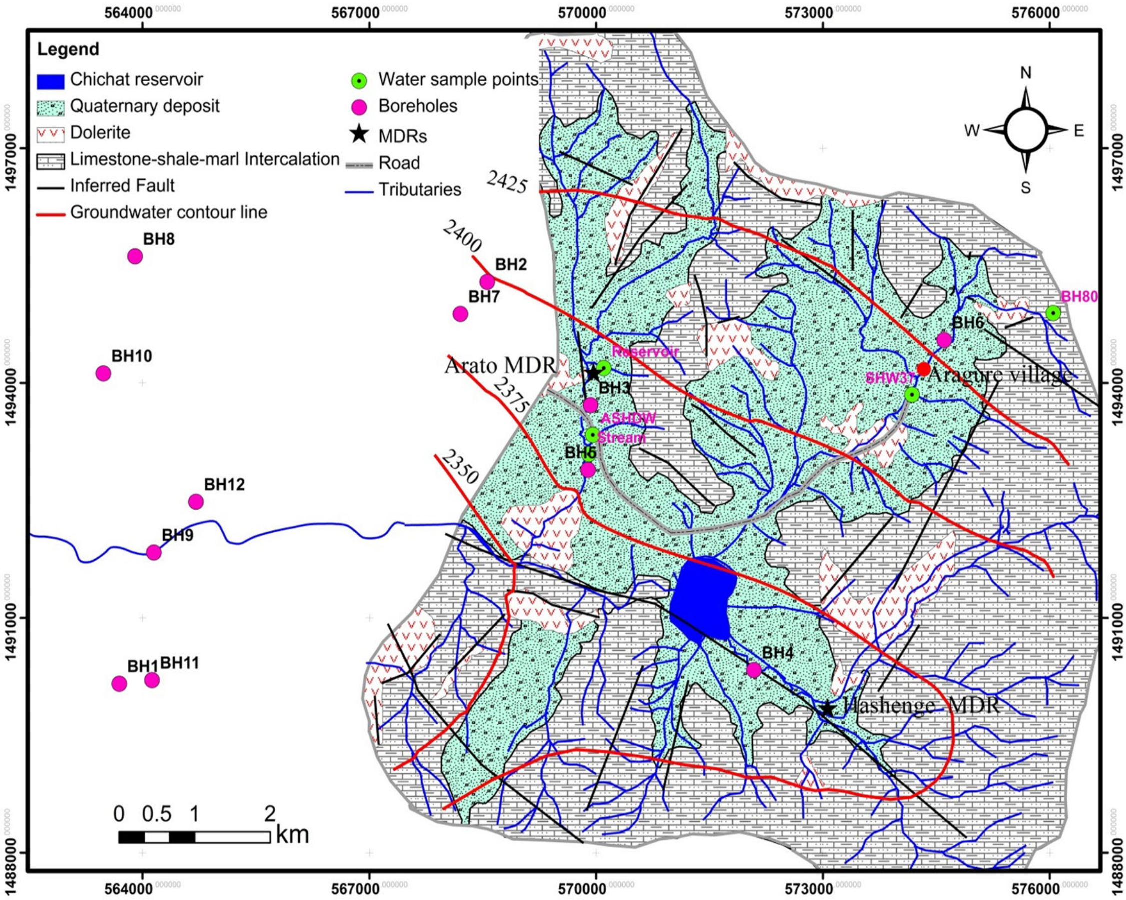

Fig. 4 Geological map of Arato MDR and its environs (modified after Berhane et al. 2013). Groundwater contour *lines* are indicated and labeled in m.a.s.l

clay to coarse sand with minor inclusions of gravel (Berhane et al. 2013). The central foundation of the MDR is covered by this superficial materials underlying by limestone-shale-marl intercalation.

These deposits cover the central part of the reservoir and downstream of Arato MDR (Berhane et al. 2013). Recently, shallow hand dug wells are excavated into the Quaternary deposits on the downstream side of the reservoir, to harvest subsurface water for various uses. The deposits were found to be pervious and water bearing in areas where sand and gravel (resulting from weathering of dolerite and limestone-shale-marl intercalation) predominate and along its contact with the underlying bedrock.

Dolerite

Dolerite forms swarms of dykes, sills and irregular bodies within Mesozoic sedimentary sequences with varying width and length between few meters to several kilometers. It is characterized by dark grey colour, and exfoliation/spheroidal weathering (peeling off the outer layers of the rock surface) and massive nature. Degree of weathering of this rock varies from place to place; it is completely weathered along the contact with limestone-marl-shale and fault zones. The grain size of this unit ranges from medium to coarse. Generally, the degree of weathering of dolerite decreases with depth (Berhane et al. 2013). This rock unit is exposed on the right abutment (west) and south of the MDR (Figs. 4, 5). The thickness of the dolerite in the right abutment (west side) is not well documented. The sills have observed to be sub-horizontal following the bedding plane of the sedimentary rocks. Fractured and weathered dolerite sills and dykes with sufficient extent and with suitable topographic feature can form potential aquifers.

From the well log and field information in the area, the thickness and physical characteristics of the weathered and fractured layer of the dolerite intrusions are not uniform throughout the catchment where these intrusions are exposed. The thickness ranges from about 30 to 250 m in surface exposures in the area. It was also observed that most of the dolerite outcrops were intruded in between the sedimentary formations, but in the vertical section or log of

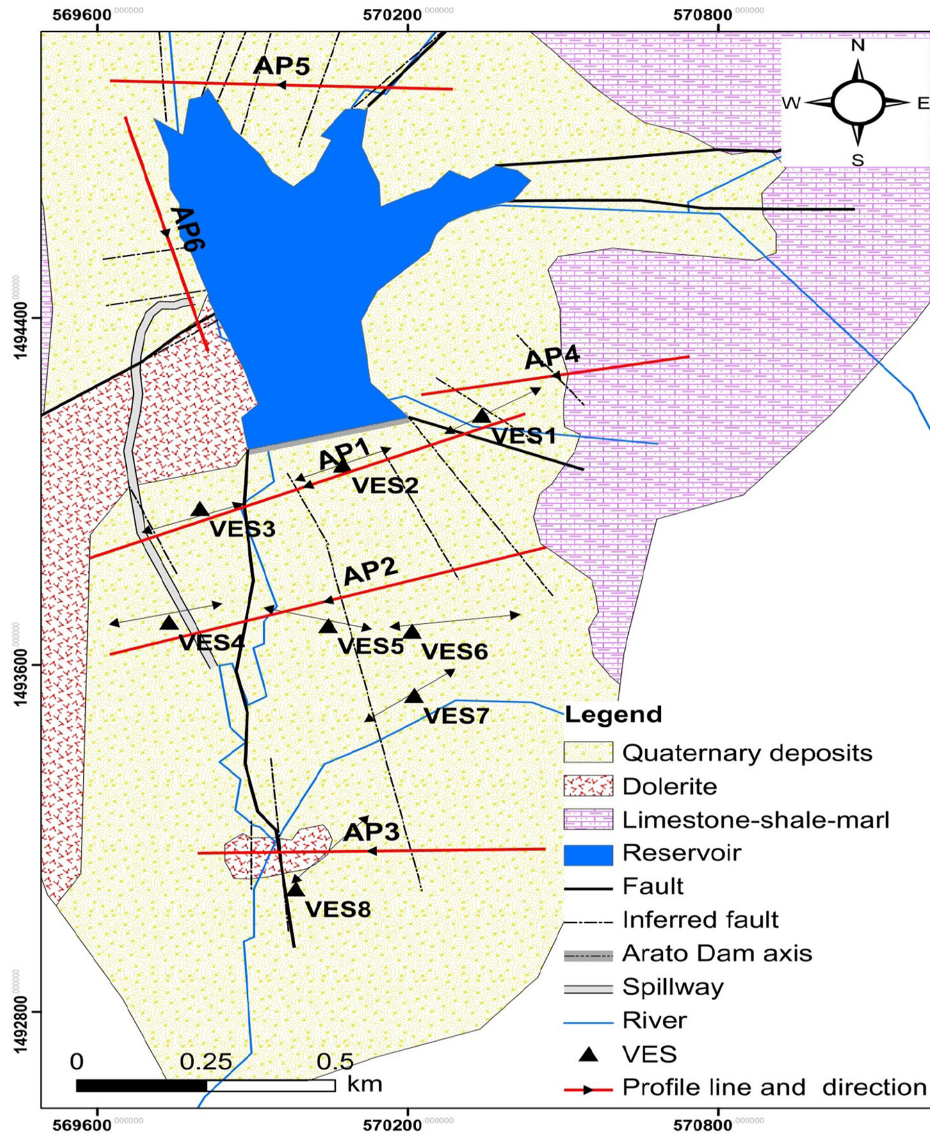

Fig. 5 Geological map of Arato MDR. Locations of VES and ERP are shown. UTM Zone 37°N coordinate system and *lines* with *double arrow* indicates electrode alignment direction for the VES

some wells a thickness of up to 33 m (Fig. 6) is observed. Although the degree of both weathering and fracturing is relatively high at the upper part of the dolerite intrusions, the aquifer capacity of this part is low. This is due to the effect of the clayey weathering products from the overlying sedimentary rocks. The geological log from most wells depicts that the type of the aquifer within dolerite intrusion in the area is characterized by confined and unconfined aquifers (Figs. 6, 7).

Limestone-shale-marl intercalation

This formation occupies an extensive area around Arato MDR and its environs. Limestone-shale-marl intercalation unit, which is part of the Agula Shale, covers large part of the area. Its colour is variegated (lateral and with depth); it varies between light grey, yellowish and brownish. This rock unit has an average thickness of about 30 m (Gelena 2013) in the area. From this intercalation unit, the limestone subunit is relatively thicker than the others. These rocks are vastly affected by weathering and tectonic activities. Due to faulting and dolerite intrusion the bedding plane of this rock unit is tilted towards east (Berhane et al. 2013). Joints are prominent on the east of Arato MDR. The degree of weathering diverges from place to place: completely weathered along the contact with dolerite, due to the roasting/baking effect of the dolerite intrusion and along fault zones, and slightly weathered at the north of the study area. A sinkhole with a significant diameter is observed on the eastern side (left abutment) of Arato reservoir. The presence of gypsum is observed in drilling logs in the area (Fig. 6).

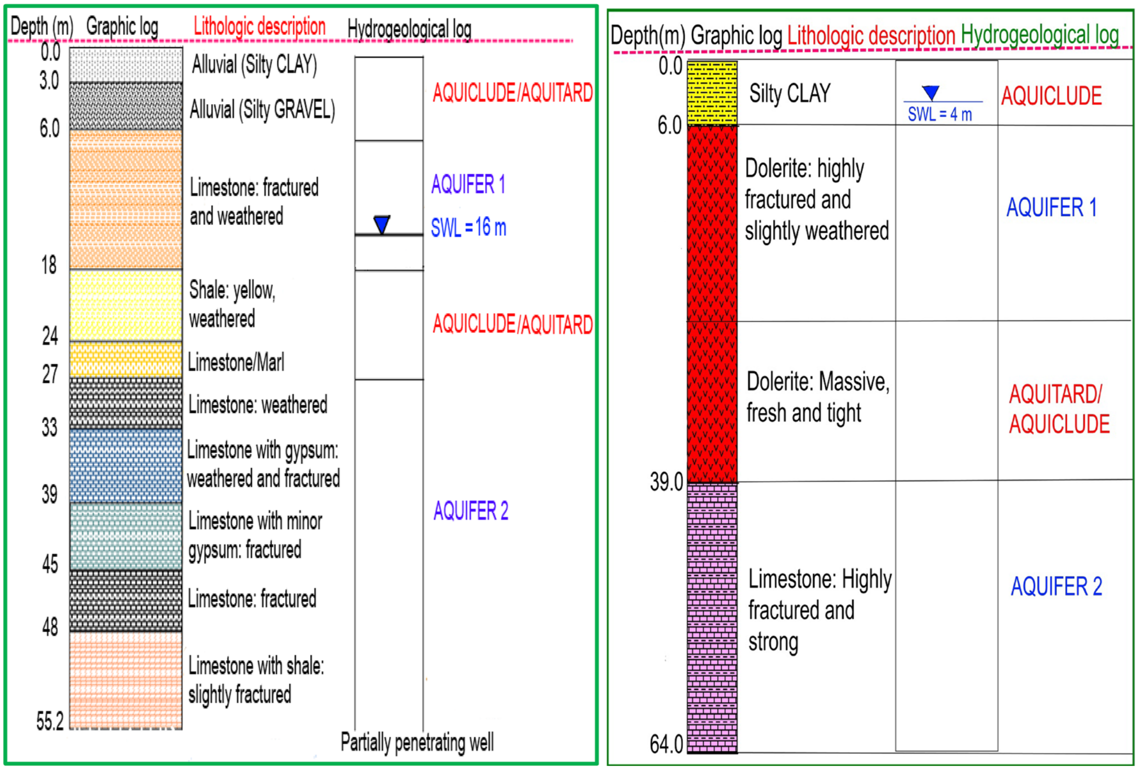

Fig. 6 Lithological and hydrogeological log of a drilled well in limestone-shale-marl intercalation and dolerite units near Arato MDR (modified from Kassa 2011 and Tigray Water Works Construction Enterprise, TWWCE). *Left* BH10 and *right* BH5 in Fig. 4

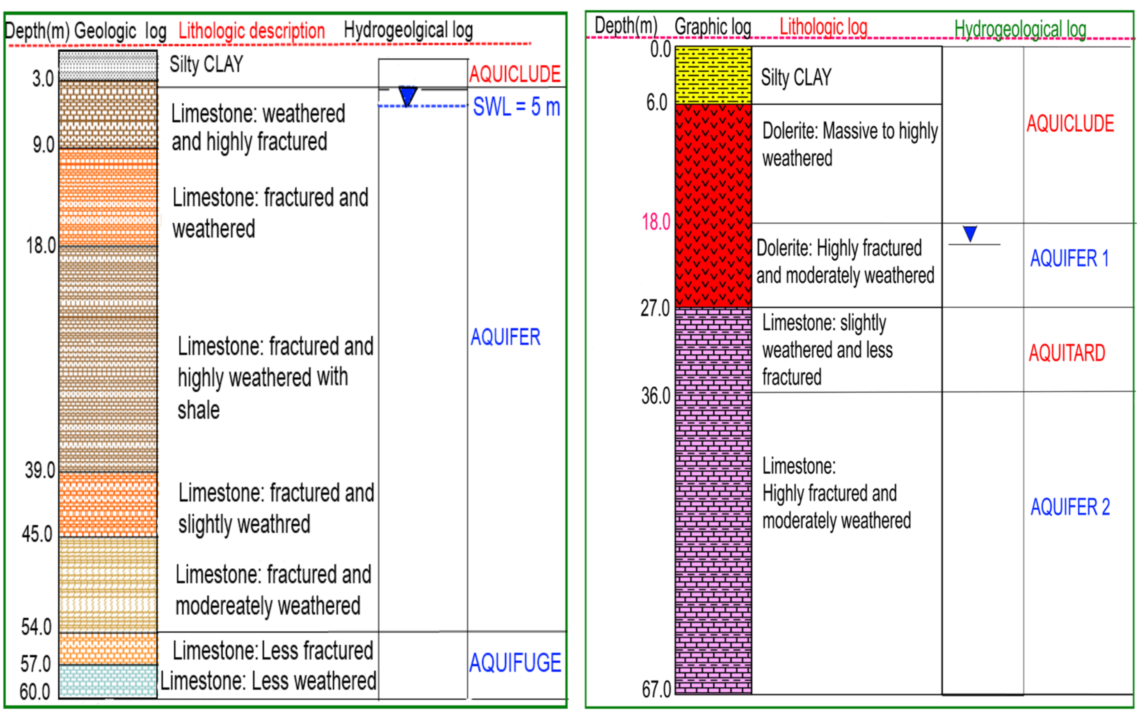

Fig. 7 Lithological and hydrogeological log of a drilled well in limestone-shale-marl intercalation and dolerite unit near Arato MDR (modified from Kassa 2011 and Tigray Water Works Construction Enterprise, TWWCE). *Left* SHW37 and *right* BH3 in Fig. 4

Figure 6 portrays the geological and hydrogeological log illustrating the typical aquifer systems in the area. The limestone layer is hard and well jointed having highest infiltration rate, while the shale and marl layers are soft and powdery having lower infiltration rate. Because of the inter-bedded fractured limestone and shale layers, groundwater exists under semi-confined condition in this unit. Boreholes drilled in this unit elsewhere are artesian (Yihdego 2003). The relatively high permeability of this unit is due to its disturbance by the dolerite intrusion and tectonic joints and dissolution cavities in the limestone layer. The highly jointed parts of the limestone bed favor groundwater storage and movement.

Wells drilled in the limestone-shale-marl intercalation unit have an average hydraulic conductivity and transmissivity value of 12.3 m/day (1.42×10^{-2}cm/s) and 186 m^2/day, respectively. In areas where it is thick, the limestone is the main aquifer system with highest hydraulic conductivity values ranging from 18.6 to 57.5 m/day (2.15 to 6.66×10^{-2}cm/s) and transmissivity value of 336–403 m^2/day (Yihdego 2003).

From the hydrogeological characteristics of the limestone-shale-marl intercalation it is clear that when it exists at foundation, abutments and reservoir, water losses will occur and water will drain toward downstream leaks and seeps or vertically downward to feed the aquifer system. This phenomenon is very common in many MDRs in northern Ethiopia, including Arato MDR. In many MDR water flows in concentrated paths and emerges downstream creating streams, or water infiltrates at the reservoir bottom through the permeable materials.

Geological structures

The main geological structures observed in the study area are faults and joints. The area is affected by minor and major faults. Mekelle Fault with strike direction of NW–SE is the major fault in the area (Berhane et al. 2013; Fig. 4). Most of the tributaries of Arato River are controlled by minor geological structures. Inferred faults are identified in study area, within limestone-shale-marl intercalation and between limestone-shale-marl intercalation and dolerite rocks. Most of the faults in this study area have a NE–SW orientation (Fig. 4).

The area is characterized by joints with NW–SE and NE–SW prevailing strike direction. These geological structures are more dominant in the limestone-shale-marl intercalation unit. According to the discontinuity histogram of Berhane et al. (2013), the dominant strike of discontinuities on east and west abutment of the Arato micro-dam is NW–SE and WNW–ESE, respectively.

Hydrogeophysical investigations

Vertical electrical sounding (VES)

A total of 8 VES (Fig. 5) with Schlumberger array were conducted at the MDR to decipher the vertical variation at the point of soundings. Brief summary of the interpretations of the VES is given in Table 1.

VES data were interpreted based on local geological information, observation of natural outcrops and shallow hand dug wells downstream of the MDR. The interpreted true resistivity values vary from 5.74 to 1155 Ωm (Table 1). This wide variation in resistivity values is mainly attributed to the variation in geological units, degree of fracturing, weathering and water content. In addition to the overall geology, during interpretations it was recognized that topmost dry soils have greater resistivity in comparison to saturated soils (Zohdy et al. 1974); weathered and discontinuous rocks have lower resistivity than massive and compacted rocks.

Based on the results of the interpretation of VES1 and VES2 the saturated and pervious subsurface materials extend up to a depth of 14.5 m to more than 16 m. Considering the geology of the area the pervious layers are correlated to and limestone-shale-marl intercalations (44.6–83.2 Ωm) with top clay cover (Quaternary deposit) (9.4 Ωm) and underlain by less weathered and fractured rocks of the same unit with resistivity values ranging from 306 to 385 Ωm. Generally, weathering and degree of discontinuity or aperture decreases with increasing depth due to overburden pressure. Permeability and porosity in the weathered zone of rocks vary throughout the rock profile. Porosity generally decreases with depth while permeability possesses a complicated relationship, depending on the extent of fracturing and the clay content (Chilton and Foster 1995; Yusuf et al. 2011).

VES 1 and 2 are located at the downstream side of the dam foundation; hence the leakage beneath the dam body can be ascribed to the fractured and weathered limestone-shale-marl intercalation unit. Leakage becomes more serious in areas where fractured limestone dominates the intercalation unit than where shale or marl dominates.

VES 3, 4 and 8 are located on dolerite unit overlain by Quaternary deposits of variable thickness. The first geoelectric layer was interpreted to be moist to dry top clay soil with a thickness that varies from 1.2 to 4.4 m, while the resistivity ranges from 12.3 to 117 Ωm. The second geoelectric layer was interpreted to be saturated and completely to slightly weathered dolerite with variable degree of fracturing. This unit and the limestone-shale-marl intercalation are considered as the pervious aquifer, responsible for the circulation and

Table 1 Summary of the hydro-lithological interpretation of VES data from Arato MDR

VES	Layer (*N*)	Resistivity (Ωm)	Thickness (m)	Interpretation
1	1	83.2	6.9	Fractured, weathered and partially saturated limestone-shale-marl intercalation/Quaternary deposit
	2	58.0	7.6	Fractured, weathered and saturated limestone-shale-marl intercalation
	3	385.0	15.7	Slightly fractured limestone
	4	143.0		Limestone-shale-marl intercalation
2	1	9.4	3.6	Moist top clay soil/Quaternary deposit
	2	44.6	12.5	Weathered, fractured and saturated limestone-marl intercalation
	3	306.0	34.5	Slightly fractured limestone
	4	84.9		Shale dominant limestone-shale-marl intercalation
3	1	117.0	4.4	Dry top clay soil/Quaternary deposit
	2	123.0	24.2	Fractured and slightly weathered dolerite
	3	238.0		Slightly fractured dolerite
4	1	17.0	1.2	Moist top clay soil/Quaternary deposit
	2	6.0	3.3	Saturated and completely weathered dolerite
	3	44.2	15.3	Saturated, weathered and fractured dolerite
	4	242.0		Fractured and slightly weathered dolerite
5	1	9.5	3.1	Moist top clay soil/Quaternary deposit
	2	50.3	18.7	Saturated, weathered and fractured limestone-shale-marl intercalation
	3	349.0		Fractured limestone
6	1	9.8	2.7	Moist top clay soil/Quaternary deposit
	2	52.9	15.8	Weathered, fractured and saturated limestone-shale-marl intercalation
	3	221.0		Fractured limestone
7	1	15.2	4.6	Moist top clay soil/Quaternary deposit
	2	35.0	14.0	Saturated, weathered and fractured limestone-shale-marl intercalation
	3	346.0		Fractured limestone
8	1	12.3	1.8	Moist top clay soil/Quaternary deposit
	2	5.7	3.0	Completely weathered and saturated dolerite (clayey soil)
	3	1155.0		Compacted dolerite

movement of the leakage water from the reservoir. Some hand dug wells have been excavated in this area, after the construction of the MDR, for irrigation purposes. The water level in these hand dug wells varies from 0 (just at the surface) to 2.3 m below ground surface. The third geoelectric layer was interpreted to be slightly fractured to compacted dolerite which is considered as aquitard/impervious unit with resistivity values that range from 238 to 1155 Ωm. It is noteworthy to mention the shallow depth (only 4.8 m, Table 1) of the pervious layer and very high resistivity value of the third geoelectric layer or fresh dolerite (1155 Ωm) at VES 8. This result is explained by the fact that VES8 is located immediately near or next to natural outcrop of dolerite where its weathered mantle is removed by erosion (Fig. 5).

VES 5, 6 and 7 are located on the limestone-shale-marl intercalation unit overlain by Quaternary deposits of clayey types comparable to VES 1 and VES 2 (Fig. 5). The first geoelectric layer which is the moist top clay soil varies in thickness from 2.7 to 4.6 m, while the resistivity ranges from 9.5 to 15.2 Ωm. The second geoelectric layer was interpreted to be the saturated, weathered and fractured limestone-shale-marl intercalation unit which is again responsible for the circulation of subsurface water. Its thickness varies from 14 to 18.7 m while the resistivity values range from 35 to 52.9 Ωm. The third geoelectric layer is a resistive unit with resistivity values that spread between 221 and 349 Ωm, which depict the presence of slightly fractured limestone dominated intercalation unit. This unit is assumed to be an aquitard or impervious layer.

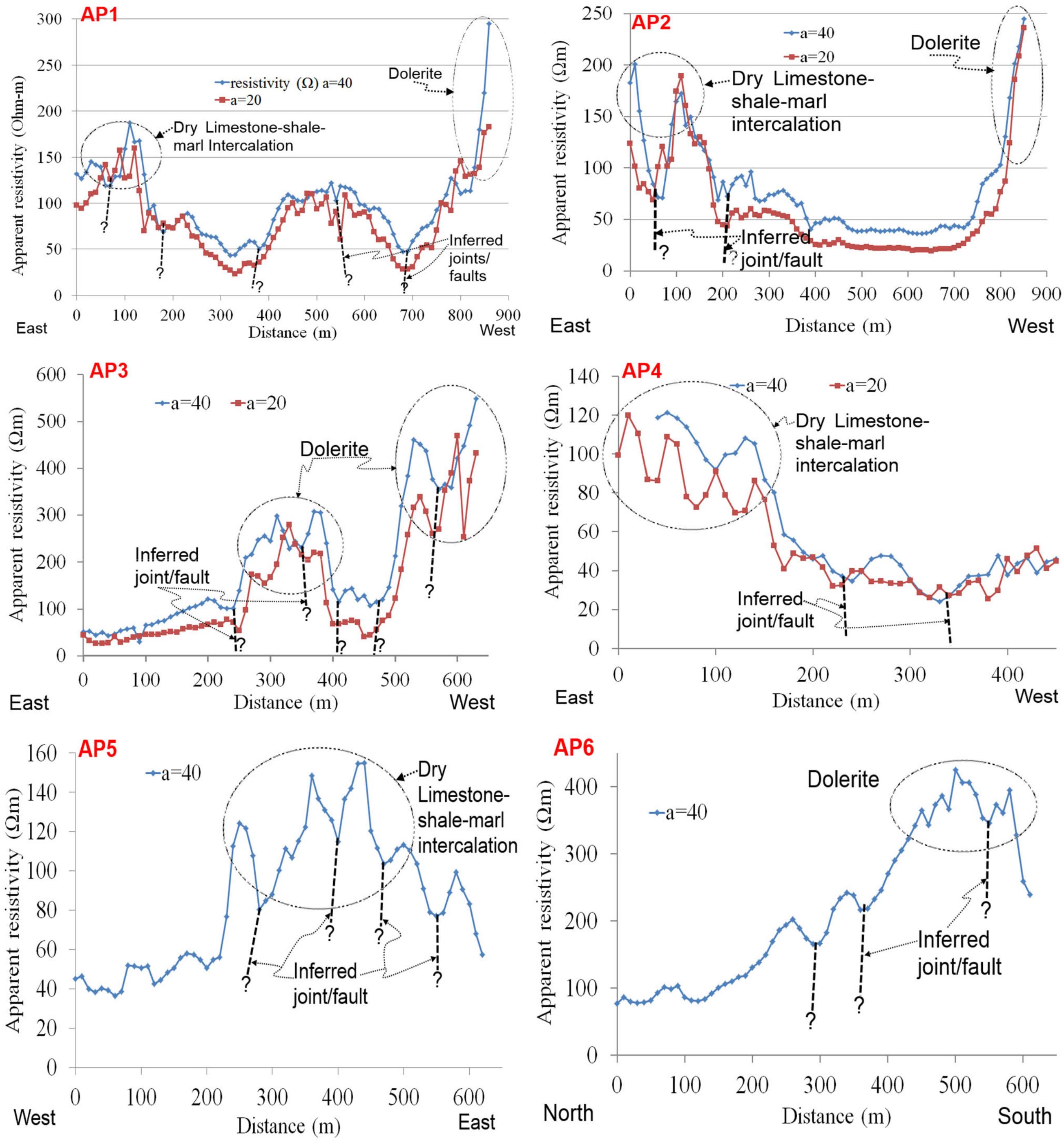

Fig. 8 Graphical plot of ERP (apparent resistivity versus horizontal distance) for the six profile *lines* with lithological and structural interpretations. For localization of profile *lines* see Fig. 5

Electrical resistivity profiling (ERP)

A total of 6 ERP measurements (three on the downstream side, one at the upstream, one at the left abutment (east) and one at the right abutment (west) of Arato MDR, Fig. 5) were conducted to identify lateral variations in resistivity along the profile lines. The graphical representation of the ERP measurements and interpretations are depicted in Fig. 8.

Due to the fact that ERP allows the detection of lateral changes in the resistivity of the subsurface materials, the presence of fracture zones and the degree of saturation of the ground can be determined (Kirsch 2009). The presence of water in a pore space decreases the resistivity of the rock, thus profiling can be used to give an indication of water level depth (Vandecasteele et al. 2011) and leakage zone, which can be used in revealing the leakage path from the reservoir. The ERP data of the study area were interpreted qualitatively (Zohdy et al. 1974) from the plot of apparent resistivity and horizontal distance (Fig. 8).

The discontinuities that intersect the dam axis, dipping toward downstream are the most favourable for leakage of water from MDR (Berhane et al. 2013). Vandecasteele et al. (2011) noted that seepage via the rock masses usually passes through the discontinuities.

The measured resistivity values of ERP data range from 19.3 to 548.5 Ωm. Based on the resistivity contrast of ERP data, some joints/faults were interpreted (Figs. 5, 8). Profile lines AP1, AP2 and AP3 were executed on the downstream side of the reservoir parallel to the dam-axis (Fig. 5) with a horizontal distance of 860, 850 and 630 m from east side to west side, respectively (Fig. 8). Profiles AP1 and AP2 show more or less similar patterns with higher apparent resistivity on the west and east sides and lower resistivity in the central part of the profile. This large resistivity variation is attributed to variation in degree of saturation, weathering and fracturing and rock type. The high resistivity on the west side of the profiles was interpreted as dolerite based on the local geological map and direct field observation (Figs. 5, 8), while the higher resistivity on the east side was interpreted as dry limestone-shale-marl intercalation.

The dolerite and limestone-shale-marl intercalation units are outcropped at the western and eastern part of these profiles where high resistivity was measured. The central part of the profiles with relatively lower apparent resistivity was interpreted as saturated weathered and fractured limestone-shale-marl intercalation. This zone is assumed to be the leakage path from the reservoir. Multiple joints/fractures with relatively lower apparent resistivity were also interpreted along these profiles due to greater proportion of water infiltrating along these joints/fractures.

Profile AP3 shows a different pattern than AP1 and AP2 which is explained by the local geology or location of the profile line. The higher apparent resistivity at around a distance of 300 m and beyond 500 m was interpreted as dolerite (Fig. 8) whereas the low values at distances of 0–300 m and 400–500 m are attributed to limestone-shale-marl intercalation and saturated, weathered and fractured dolerite, respectively. An outcrop of dolerite was observed during the field campaigns as portrayed in Fig. 5 along the profile line. The very low values encountered along the profiles give a possible structural interpretation like minor faults/joints. The approximate orientation of the joints/faults is N–S, i.e., nearly perpendicular to the presumed leakage path.

Profile AP4 was executed on the left abutment side of the MDR with a length of 440 m and measurements were taken from east toward west direction (Figs. 5, 8). The apparent resistivity along this profile varies from 24 to 121 Ωm. This wide resistivity variation is explained by variation in degree of weathering, fracturing and moisture content. The high resistivity anomaly was interpreted to be slightly weathered and fractured limestone dominating the intercalation unit, while the low resistivity anomaly was interpreted to be highly weathered, fractured and saturated limestone-shale-marl intercalation and saturated Quaternary deposits. The apparent resistivity dropped toward the reservoir area along the profile line indicates the presence of higher moisture content.

Profile AP5 and AP6 were executed on the upstream and right side of the reservoir water body with a horizontal distance of 620 and 610 m, respectively. Based on the local geology, the higher resistivity values at AP5 were interpreted to be dry limestone-shale-marl intercalation, while those at AP6 were interpreted as dolerite. Measurements collected near the reservoir water body and at small creeks and depressions were relatively low, which is explained by the presence of moisture from the reservoir water along joints and fractures (Fig. 8).

Hydrochemistry

Interpretation of the chemical constituents of water can provide insights into surface–groundwater interactions or surface water-aquifer connectivity. Dissolved constituents can be used as environmental tracers to track the movement of water. Some of the commonly used environmental tracers include parameters such as the major anions and cations (e.g. calcium, magnesium, sodium, chloride and bicarbonate) (Brodie et al. 2007).

Chemical composition of water provides additional information on its origin and geochemical evolution, facilitating the differentiation between reservoir and aquifer waters or a mixture of those waters. Groundwater can have a chemistry that is distinctly different from the streams and leakages from surface reservoirs, and these characteristics can be used as indicators to discriminate groundwater discharge from leakage water from surface reservoirs.

Three water samples collected from reservoir, shallow hand dug well (ASHDW) and stream were analyzed for major cations and anions. In addition results of chemical analyses from boreholes (SHW37 and BH80) were obtained from existing archives from the area (Fig. 4). All the results of the chemical analyses are illustrated in the form of vertical column diagrams (Piper trilinear diagram and Stiff diagrams, Fig. 9; Table 2). Brodie et al. (2007) pointed out that Piper diagram has the advantage of

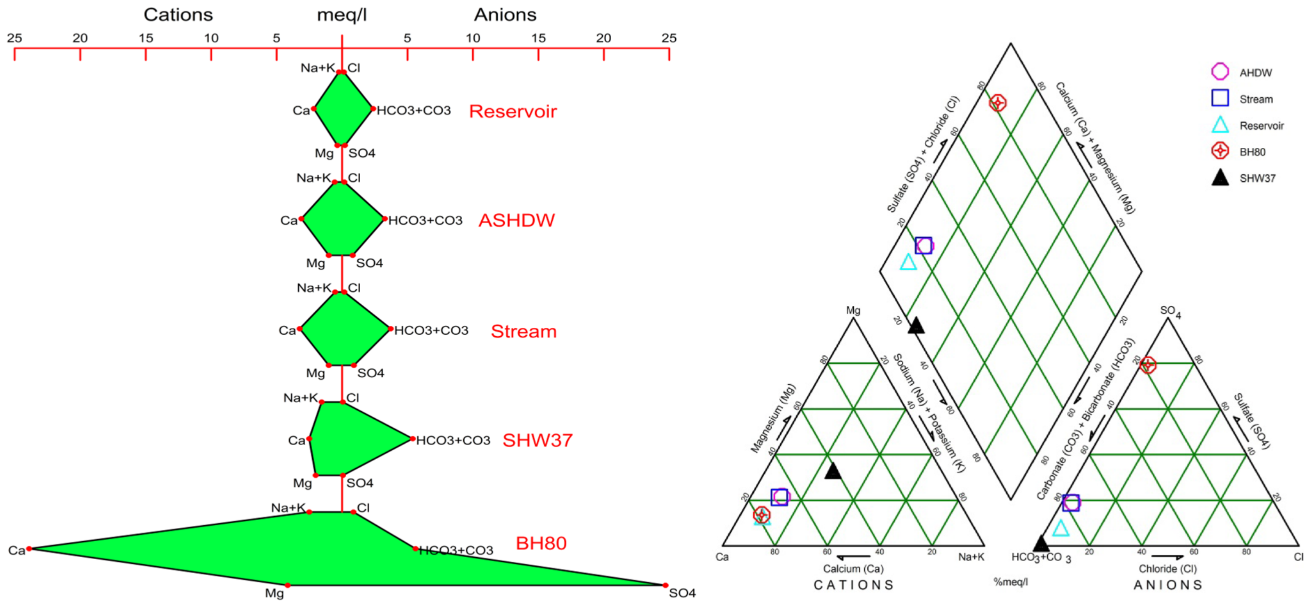

Fig. 9 Stiff and Piper diagrams for reservoir, shallow hand dug well, stream and borehole (SHW37 and BH80) water samples

Table 2 Summary of the hydrochemical data from Arato MDR and its environs

Code	East (mE)	North (mN)	Elev (m)	EC (mS/cm)	TDS (mg/l)	pH	Ca^{2+} (mg/l)	Mg^{2+} (mg/l)	Na^{+} (mg/l)	K^{+} (mg/l)	HCO_3^{-} (mg/l)	Cl^{-} (mg/l)	SO_4^{2-} (mg/l)	NO_3^{-} (mg/l)
Reservoir	570,103	1,493,125	2424	292	228.80	7.61	43.35	4.35	3.50	3.50	145.20	4.98	10.53	12.74
ASHDW	569,958	1,493,336	2398	436	351.42	7.70	62.30	12.30	12.30	1.03	199.50	6.17	38.90	18.75
Stream	569,905	1,493,090	2393	448	366.44	7.82	64.85	12.35	11.50	1.17	226.90	6.13	43.28	0.08
SHW37	574,181	1,493,850	2416	1037	739.53	6.18	50.30	24.50	12.60	39.60	329.40	2.00	3.20	0.82
BH80	576,048	1,494,893	2480	2350	1404.90	7.55	478.80	50.49	55.00	4.40	342.60	30.72	1187.00	3.96

showing a large number of analyses in one plot to define distinct populations or trends.

It can be seen from Fig. 8 that the shape of the Stiff diagrams and localizations in the Piper diagram (interwell analysis) clearly indicate that samples ASHDW and Stream have chemical compositions similar to the reservoir water, whereas the other groundwater samples (SHW37 and BH80) do not. This information indicates that the source for the ASHDW and the Stream water downstream of Arato reservoir is water leaking from the reservoir. The residence times for water samples from ASHDW and Stream appear short in comparison to the water samples from boreholes, resulting in little rock-water interaction compared to the reservoir water. Only limited calcite dissolution has occurred in ASHDW and Stream, compared to the reservoir water, raising Ca^{2+} and HCO_3^{-} to some extent. Total dissolved solids in ASHDW and Stream is therefore somewhat increased (~360 mg/l), compared to reservoir water (229 mg/l). However, the unaffected groundwater in the area is much more mineralized, due to stronger carbonate dissolution (raising HCO_3^{-}), and cation exchange (raising Mg^{2+} and Na^{+}). The raised concentration of K^{+} in SHW37 could be attributed to clay resulted from weathering of shale and dolerite. In BH80 dissolution of gypsum from the limestone-shale-marl intercalation unit results in high SO_4^{2-} and Ca^{2+} concentrations, and a high mineralization. The contrasting chemistry between typical groundwater of the area, compared to the shallow hand dug well and stream downstream of the reservoir, which are very comparable to the reservoir water, confirms our assumption that the latter water is derived from leakage from the reservoir.

The piezometric map (Fig. 4) illustrates that both SHW37 and BH80 are upgradient with groundwater levels of 2411 and 2450 m.a.s.l., respectively, with respect to the MDR, while the groundwater level in the big diameter shallow hand dug wells, that were developed after dam construction in the downstream part, the water level ranges

Table 3 Groundwater level measurements from Boreholes and big diameter Hand dug wells

Boreholes/groundwater[a]					Large diameter shallow hand dug wells/leakage water[b]			
Borehole ID	Elevation (m)	Depth (m)	Water level (m.b.g.l.)	Water level (m.a.s.l.)	Hand dug well ID	Elevation (m)	Water level (m.b.g.l.)	Water level (m.a.s.l.)
BH1	2261	60	21	2240	AHDW1	2409	2.3	2406.7
BH2	2410	70	11	2399	AHDW2	2402	1.1	2400.9
BH3	2409	67	21	2388	AHDW3	2402	0.3	2401.7
BH4	2377	62	19	2358	AHDW4	2402	0.5	2401.5
BH5	2391	64	4	2387	AHDW5	2400	1.2	2398.8
BH6	2436	58	5.5	2430.5	AHDW6	2399	1.2	2397.8
BH7	2405	63.5	18	2387	AHDW7	2401	1.2	2399.8
BH8	2411	72	21	2390	AHDW8	2401	1.6	2399.4
BH9	2243	70	13	2230	AHDW9 (ASHDW)	2398	0	2398
BH10	2321	55.2	18	2303				
BH11	2288	60	9	2279				
BH12	2267	51	16.7	2250.3				
BH80	2480	60	30	2450				
SHW37	2416	60	5	2411				

For locations see Figs. 4 and 10

[a] All are drilled boreholes

[b] All are excavated manually and occasionally by excavator, diameter ranges from 2 to 5 m and depth ranges from 3 to 8 m

from 2397.8 to 2406.7 m.a.s.l. (Table 3). This confirms that the water quality in SHW37 and BH80 cannot be affected by the reservoir. From the piezometric map it is possible to identify a main direction of the groundwater flow from NE to SW. In addition, the groundwater level measurements illustrate the distinction between the boreholes around the MDR and shallow hand dug wells immediately downstream of the MDR. From Table 3 it is clear that there are two groups of groundwater levels around the MDR. The boreholes (BH3 and BH5) have water levels <2388 m.a.s.l. while the large diameter shallow hand dug wells have water levels >2397.8 m.a.s.l. This can be explained by the fact that the reservoir water is feeding the nearby shallow aquifer and hence affects the water levels close to the reservoir. Prior to reservoir construction there were no shallow hand dug wells next to the MDR. At present, test pits excavated to similar elevation as the hand dug wells near Arato MDR in adjacent catchments, and in the same catchment but far from the influence of reservoir, were found to be dry. This implies that the existence of shallow water levels downstream of the MDR is related to the leakage phenomenon from the reservoir. Local residents reported that swamps or wetlands exist on the downstream side of the MDR when reservoir level rises following the rain season. This situation was confirmed during our field visit in September–November 2014, in which irrigated land was abandoned due to the presence of small swamps which were not existent prior to dam construction.

Leakage zone and path

The need to reduce the risk of failure or to control water loss has led to costly remedial measures that are planned and executed without a comprehensive understanding of the leakage problem, its path and mechanism. Contreras and Hernandez (2010) reported that a large quantity of technical and economic resources are spent without positive outcomes due to the lack of adequate characterization to determine water origin, preferential paths, recharge zones, and transit time. A lack of appropriate leakage investigation and monitoring can result in maintenances or remedial measures that are unsuccessful in controlling or reducing leakage. Sufficient and complete information about the engineering geology and hydrogeology of the problem that allows understanding of the leakage zones and path is crucial.

Based on geological, geophysical, hydrogeological and hydrochemical methods, it was possible to delineate the leakage zone and its path (Figs. 10, 11). The leakage path is from the central and left reservoir bank/foundation and directs in a slight curved shape toward the downstream creating a flowing stream and feeding the shallow aquifer starting from the toe of the dam. Eight shallow hand dug

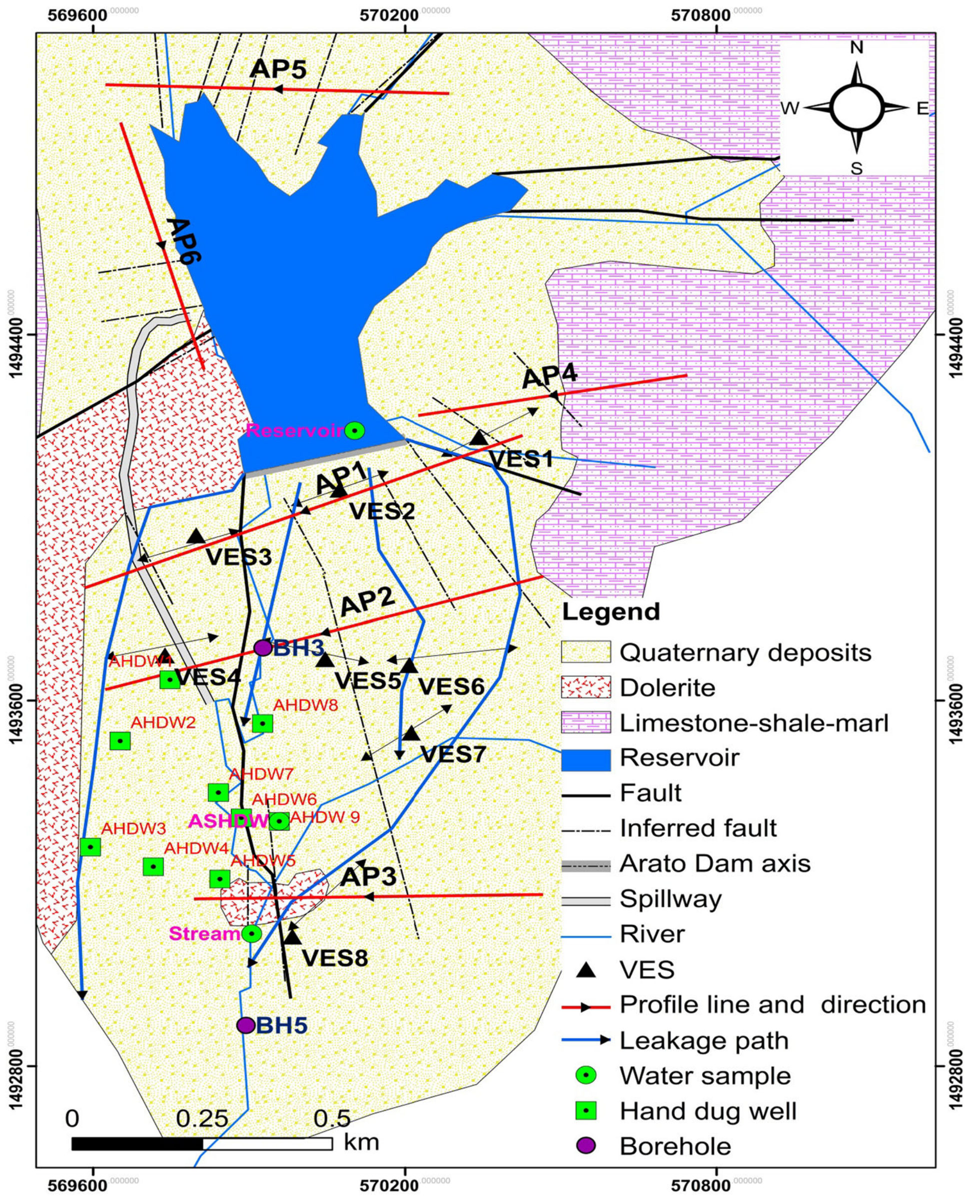

Fig. 10 Leakage zone and path from the reservoir. Large diameter hand dug wells and boreholes next to MDR and water sample points are indicated

wells were excavated in this area to exploit the infiltrated water from the reservoir for small household irrigation and drinking purposes. Field observations and data analysis/interpretations show that the limestone-shale-marl intercalation unit could be responsible and the main cause for the leakage. This unit is affected by discontinuities of syngenetic (developed contemporaneously with the rock) and epigenetic (developed after the formation of the rock) forms, while the dolerite unit is less affected by the discontinuities. The leakage path and mechanism have been analyzed and diagnosed with the different methods mentioned. Geophysical methods (VES1 and VES2) show that the pervious zone in the central foundation and left abutment extends to a depth of about 14 to 16 m below surface. The low resistivity geological formation in the downstream side of the dam extends up to a depth of about 20 m which is explained by presence of discontinuities, weathering and saturation.

The reservoir lies entirely within the Quaternary deposit underlain by the leaky limestone-shale-marl intercalation of the Agula Shale, although the southwest reservoir rims and abutment are composed of dolerite unit. Due to this situation, controlling the quantity of leakage that occurs through this unit may be difficult and expensive by an upstream or reservoir blanket. Installation of a cut-off wall at the upstream toe of the dam could be the best option. Proper design and construction, exploiting and managing the shallow hand dug wells in the downstream of the dam

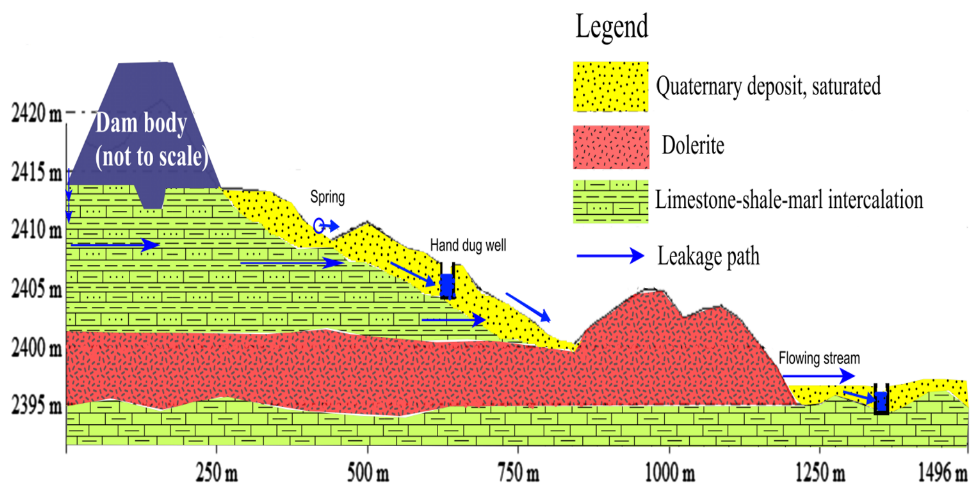

Fig. 11 Simplified conceptual geological model illustrating the mechanism of leakage in two dimensional view. Cross-section taken from dam body to downstream direction (N–S). *Horizontal axis* is distance and *vertical axis* is elevation above sea level taken from digital elevation model. Dam body is sketched on *top*

may be considered as a second alternative solution to the problem.

Conclusion and recommendation

Arato MDR is situated on three lithological units: Quaternary soil deposits, dolerite and limestone-shale-marl intercalation unit. The geological, hydrogeological, hydrogeophysical and hydrochemical data analysis reveals the presence of hydraulic connection between the impounded reservoir and the downstream leakage discharge zone. The limestone-shale-marl intercalation unit of Agula Shale is found to be the leaky formation and responsible for the inefficient performance of the project in terms of water loss via leakage.

The relatively low resistivity data recorded up to a depth of 16 to 20 m in the downstream side of the dam were inferred to be generally due to highly conductive material, likely the water saturated and pervious limestone-shale-marl intercalation unit and Quaternary soil deposits, and partly due to deep weathering of the dolerite unit. The highly resistive materials in the area were found to be massive dolerite and dry limestone dominated intercalation unit (Agula Shale). Hydrochemical data from reservoir water, from downstream shallow hand dug well and stream water confirmed that these waters are of the same origin, such that the source for the subsurface and stream water is from the impounded reservoir.

The available hydrogeological information concerning the limestone-shale-marl intercalation unit confirms it to be the main water bearing formation in the area in the form of a multi-layer aquifer system.

Installation of a cut-off wall at the upstream toe of the dam could be the possible solution to minimize the leakage problem underneath the dam foundation and left abutment. In addition the installation of a grout curtain up to the depth of fresh dolerite and limestone-shale-marl intercalation unit can be used as a remedy to prevent leakage. From the geophysical survey, the depth to tight and massive formation was estimated to be in the range of 16–20 m. It is generally recommended to perform drilling and Lugeon test to check the hydraulic conductivity and groutability of the rock units. As an alternative, proper utilization of the water in the shallow wells from the leakage zone in the downstream part of the MDR may also be conceived as a target without incurring additional costs of maintenance.

Future planning, design and construction of MDRs in the area shall be based on sound understanding of the geomorphology/topography, geology, geo-hydrology and engineering geology of the site.

Acknowledgments The financial support to conduct the fieldwork was obtained from MU-NORAD III project through local research Grant with Registration Number CNCS/MU-UMB/05/2012. Ghent University, Laboratory for Applied Geology and Hydrogeology and Mekelle University are highly acknowledged for various assistances, water quality analysis and scholarship grant from Special Research Fund (BOF) of the University to the first author to pursue Ph.D. research and prepare this manuscript. The authors wish to express their sincere thanks to the Flemish Interuniversity Council (VLIR) for funding the North–South-South collaboration project "Sustainability of groundwater exploitation", which contributed to this study. The authors would like to thank the Ministry of Water Resources of the Federal Democratic Republic of Ethiopia, the National Meteorological Agency of Ethiopia and Tigray Water Resources Development Bureau for providing different data sets.

References

Abdulkadir M (2009) Assessment of Micro-Dam Irrigation Projects and Runoff Predictions for Ungauged Catchments in Northern Ethiopia, Ph.D. Dissertation, Muenster University, Germany

Alene M, Jenkin G, Leng M, Darbyshir F (2006) The Tamben Group, Ethiopia: an early Cryogenian (Ca. 800–735 Ma) Neoproterozoic sequence in the Arabian-Nubian Shield. Precambrian Res 147:79–99

Appelo CAJ, Postma D (2005) Geochemistry, groundwater, and pollution (2nd edn). Balkema, Amsterdam, p 635

Arkin Y, Beyth M, Dow DB, Levitte B, Haile T, Hailu T (1971) The Geological map of Mekele area. Ministry of Mines of Ethiopia, Addis Ababa

Asrat A, Barbey P, Gleizes G (2001) The Precambrian geology of Ethiopia: a review. Afr Geosci Rev 18:271–288

Asrat A, Gleizes G, Barbeya P, Ayalew D (2003) Magma emplacement and mafic–felsic magma hybridization: structural evidence from the Pan-African Negash pluton, Northern Ethiopia. J Struct Geol 25:1451–1469

Baert R (2011) Hydrogeological investigation of the Mendae agricultural plain and the Tsenkanet reservoir (Tigray, Ethiopia). Unpublished M.Sc. Thesis, University of Ghent

Bedrosian PA, Burto BL, Powers MH, Minsley BJ, Phillips JD, Hunter LE (2012) Geophysical investigations of geology and structure at the Martis Creek Dam, Truckee, California. J Appl Geophys 77:7–20

Behailu M, Haile M (2003) Water harvesting in northern Ethiopia: environmental, health and socio-economic impacts. In: MoWR/EARO/IWMI/ILRI Workshop. International Water Management Institute, pp 185–191

Berhane G (2010) Geological, geophysical and engineering geological investigation of a leaky micro-dam in the Northern Ethiopia. Agric Eng Int CIGR J 12(1):31–46

Berhane G, Walraevens K (2013) Geological challenges in constructing the proposed Geba dam site, northern Ethiopia. Bull Eng Geol Environ 72:339–352. doi:10.1007/s10064-013-0480-9

Berhane G, Martens K, Al Farrah N, Walraevens K (2013) Water leakage investigation of micro-dam reservoirs in Mesozoic sedimentary sequences in Northern Ethiopia. J Afr Earth Sci 79:98–110

Beyth M (1971) The Geology of Central and Western Tigray. Unpub. Report. Ethiopian Institute of Geological Survey (EIGS), Addis Ababa

Beyth M (1972a) The geology of central and western Tigre. Ph.D. Thesis, University of Bon, Germany, pp 155

Bobachow A (2002) Ipi2win user's guide. Moscow State University

Brodie R, Sundaram B, Tottenham R, Hostetler S, Ransley T (2007) An overview of tools for assessing groundwater-surface water connectivity. Bureau of Rural Sciences, Canberra

Cherent T (1993) Hydrogeology of Ethiopia and water resource development. EIGS, Addis Ababa

Chilton PJ, Foster SSD (1995) Hydrogeological characterisation and water-supply potential of basement aquifers in tropical Africa. Hydrogeol J 3(1):36–49

Coker JO (2012) Vertical electrical sounding (VES) methods to delineate potential groundwater aquifers in Akobo area, Ibadan, South-western, Nigeria. J Geol Mining Res 4:35–42

Contreras IA, Hernandez SH (2010) Techniques for prevention and detection of leakage in dams and reservoirs. http://ussdams.com/proceedings/2010Proc/785-814.pdf. Accessed 04 April 2014

Desta LT (2005) Reservoir Siltation in Ethiopia: Causes, Source Areas and Management Options. Ph.D. Dissertation, University of Bonn, Germany

Döll P (2009) Vulnerability to the impact of climate change on renewable groundwater resources: a global-scale assessment. Environ Res Lett 4:035006

Dow DB, Beyth M, Tsegaye H (1971) Paleozoic glacial rocks recently discovered in northern Ethiopia. Geol Mag 108:53–59

Dubey N, Bheemalingeswara K, Tadesse N (2007) Sedimentology and lithostratigraphy of the Mesozoic successions of Mekelle Basin of Ethiopia, Northeastern Africa. Geophys Res Abstr 9

Evans AEV, Giordano M, Clayton T (2012) Investing in Agricultural Water Management to Benefit Smallholder Farmers in Ethiopia

Garland CR (1980) Geology of the Adigrat Area. Ministry of Mines, Addis Ababa Memoir No. 1, pp 51

Garrido A, Martínez-Santos P, Llamas MR (2006) Groundwater irrigation and its implications for water policy in semiarid countries: the Spanish experience. Hydrogeol J 14:340–349

Gelena SK (2013) Gephysical investigation of groundwater parameters in an agricultural area (Abraha Atsbeha) and leaking Micro-Dam reservoir (Arato Dam) in Tigray, Ethiopia. M.Sc. Thesis. Ghent University and Vrije Universiteit Brussel, Belgium

Gonzalez-Quijano M (2006) Groundwater Modelling of the Tsinkanet Catchment: a MODFLOW Approach to Evaluate the Impact of Small Reservoirs on Groundwater Recharge. M.Sc. Thesis University of Ghent and University of Brussels, Belgium

GWP (2010) Global water security Global Water Partnership Secretariat. (Drottninggatan 33, SE-111 51 Stockholm, Sweden)

Haregeweyn N, Poesen J, Nyssen J, Verstraeten G, de Vente J, Govers G, Deckers S, Moeyersons J (2005) Specific sediment yield in Tigray-Northern Ethiopia: assessment and semi-quanttative modelling. Geomorphology 69:315–331

Haregeweyn N, Poesen J, Nyssen J, De Wit J, Haile M, Govers G, Deckers S (2006) Reservoirs in Tigray (northern Ethiopia): characteristics and sediment deposition problems. Land Degrad Dev 17:211–230

Houben GJ, Weihe U (2010) Spatial distribution of incrustations around a water well after 38 years of use. Ground Water 48:53–58

Kassa G (2011) Aquifer characterization and groundwater quality evaluation for irrigation, Unpublished M. Sc. Thesis, Mekelle University, Ethiopia

Kazmin V (1972) The geology of Ethiopia. Ethiopian Institute of Geological Surveys. Note No. 821-051-12, pp 208

Kirsch R (2009) Petrophysical properties of permeable and low permeable rocks: In: Kirsch (eds) Groundwater geophysics: a tool for hydrogeology. Springer, Berlin

Laio F, Tamea S, Ridolfi L, D'Odorico P, Rodriguez-Iturbe I (2009) Ecohydrology of groundwater-dependent ecosystems: 1. Stochastic water table dynamics. Water Resour Res 45:1–13

Levitte D (1970) The geology of central part of Mekelle sheet (ND37-11). Ethiopian Institute of Geological Survey. Note No. 821-201-12, pp 66

Lowrie W (2007) Fundamentals of Geophysics, 2nd edn. Cambridge University Press, New York

Massoud U, Santos F, Khalil MA, Taha A, Abbas AM (2010) Estimation of aquifer hydraulic parameters from surface geophysical measurements: a case study of the Upper Cretaceous aquifer, central Sinai, Egypt. Hydrogeol J 18:699–710. doi:10.1007/s10040-009-0551-y

Nedaw D, Walraevens K (2009) The positive effect of micro-dams for groundwater enhancement: a case study around Tsinkanet and Rubafeleg area, Tigray, northern Ethiopia. Momona Ethiop J Sci 1(1):59–73

Nyssen J, Vandenreyken H, Poesen J, Moeyersons J, Deckers J, Haile M, Salles C, Govers G (2005) Rainfall erosivity and variability in the Northern Ethiopian Highlands. J Hydrol 311:172–187

Nyssen J, Clymans W, Descheemaeker K, Poesen J, Vandecasteele I, Vanmaercke M, Zenebe A, Van Camp M, Haile M, Haregeweyn N, Moeyersons J, Martens K, Gebreyohannes T, Deckers J, Walraevens K (2010) Impact of soil and water conservation measures on catchment hydrological response—a case in north Ethiopia. Hydrol Process 24:1880–1895

Panthulu TV, Krishnaiah C, Shirke JM (2001) Detection of seepage paths in earth dams using self-potential and electrical resistivity methods. Eng Geol 59:281–295

Pavelic P, Giordano M, Keraita B, Ramesh V, Rao T (eds) (2012) Groundwater availability and use in Sub-Saharan Africa: a review of 15 countries. Colombo, Sri Lanka: International Water Management Institute (IWMI). p 274. doi:10.5337/2012.213

Rønning JS, Ganerød GV, Dalsegg E, Reiser F (2014) Resistivity mapping as a tool for identification and characterisation of weakness zones in crystalline bedrock: definition and testing of an interpretational model. Bull Eng Geol Environ 73:1225–1244. doi:10.1007/s10064-013-0555-7

Scanlon BR, Keese KE, Flint AL, Flint LE, Gaye CB, Edmunds WM, Simmers I (2006) Global synthesis of groundwater recharge in semiarid and arid regions. Hydrogeol J 3370:3335–3370

Sharma SP, Baranwal VC (2005) Delineation of groundwater-bearing fracture zones in a hard rock area integrating very low frequency electromagnetic and resistivity data. J Appl Geophys 57:155–166

Srinivasamoorthy K, Chidambaram S, Vasanthavigar M, Anandhan P, Sarma VS (2014) Geophysical investigations for groundwater in a hard rock terrain, Salem district, Tamil Nadu, India. Bull Eng Geol Environ 73:357–368. doi:10.1007/s10064-013-0488-1

Tadesse T (1996) Structure across a possible intra-oceanic suture zone in the low-grade Pan-African rocks of northern Ethiopia. J Afr Earth Sc 23(3):375–381

Telford WM, Geldart LP, Sheriff RE (1990) Applied Geophysics, 2nd edn. Cambridge University Press, Cambridge

Tesfay H (2007) Assessment of Institutional Setup and Effect of Household Level Water Harvesting in Ensuring Sustainable Livelihood DCG Report, Mekelle

Vandecasteele I, Nyssen J, Clymans W, Moeyersons J, Martens K, Van Camp M, Gebreyohannes T, Desmedt F, Deckers J, Walraevens K (2011) Hydrogeology and groundwater flow in a basalt-capped Mesozoic sedimentary series of the Ethiopian highlands. Hydrogeol J 19:641–650

Wood WW (2002) The role of ground water in geomorphology, geology and pale climate of the southern high plains. Ground Water 40:438–447

Yihdego S (2003) Hydrogeology of Illala-Aynalem catchments with particular reference to the chemical variation and aquifer characterization, Unpublished M.Sc. thesis Addis Ababa University, Ethiopia

Yusuf SN, Joseph MV, Alkali SC, Kuku AY (2011) Determination of porous zones using vertical electrical Sounding data from basement rocks of Hussara, Askira Uba, North-Eastern Nigeria. Ozean J Appl Sci 4(2):182–189

Zohdy AAR, Eaton GP, Mabey DR (1974) Application of surface geophysics to ground water investigations. USGS